







Article

# Antifouling Potential of *Diadema setosum* and *Sonneratia lanceolata* Extracts for Marine Applications

Mujahidah Mohd Ramzi <sup>1</sup>, Nor Izzati Abd Rahman <sup>1</sup>, Nurul Najihah Rawi <sup>1</sup>, Kesaven Bhubalan <sup>2</sup> , Fazilah Ariffin <sup>2</sup> , Noor Wini Mazlan <sup>2</sup> , Jasnizat Saidin <sup>1</sup> , Muhd Danish-Daniel <sup>1</sup> , Julius Yong Fu Siong <sup>1</sup>, Kamariah Bakar <sup>1</sup>, Nor Atikah Mohd Zin <sup>1</sup>, Ahmad Khusairi Azemi <sup>1,\*</sup>  and Noraznawati Ismail <sup>1,\*</sup>

<sup>1</sup> Institute of Marine Biotechnology, Universiti Malaysia Terengganu, Kuala Terengganu 21030, Malaysia; mujahidahramzi96@gmail.com (M.M.R.); norizzati\_sakinah@yahoo.com (N.I.A.R.); najihah2995@gmail.com (N.N.R.); ijaxzt@umt.edu.my (J.S.); mdda@umt.edu.my (M.D.-D.); yongjulius@umt.edu.my (J.Y.F.S.); kamariah@umt.edu.my (K.B.); atikah@umt.edu.my (N.A.M.Z.)

<sup>2</sup> Faculty of Science and Marine Environment, Universiti Malaysia Terengganu, Kuala Terengganu 21030, Malaysia; kesaven@umt.edu.my (K.B.); fazilah@umt.edu.my (F.A.); noorwini@umt.edu.my (N.W.M.)

\* Correspondence: madkucai89@gmail.com (A.K.A.); noraznawati@umt.edu.my (N.I.); Tel.: +609-6683240 (N.I.)

**Abstract:** Marine resources such as marine invertebrates and mangrove plants favor the production of secondary metabolites that exhibit antifouling properties. These natural-derived compounds are considered environmentally friendly compared to synthetic compounds with similar activity and technological applications. The current study was conducted to determine the antifouling properties of *Diadema setosum* (DS) and *Sonneratia lanceolata* (SL) crude extracts and their incorporated paints, in addition to the identification of the metabolites involved. Both crude extracts were tested against *Pseudomonas aeruginosa* via a crystal violet assay, while the incorporated paints with 5% (SL5% and DS5%) and 10% (SL10% and DS10%) weight per volume (*w/v*) were tested in an aquarium and submerged in the seawater at Kemaman and Pulau Redang (Malaysia) for field testing. The identification of the bioactive compounds from the crude extracts was carried out using Liquid Chromatography-Mass Spectrometry (LC-MS). The results of the crystal violet assay showed that both of the crude extracts reduced the biofilm formed by *Pseudomonas aeruginosa*. The marine bacteria growths contained in natural seawater were inhibited the most by SL5%, followed by DS5%, DS10%, and SL10% in the aquarium testing. Based on the photographic observation, all of the paints incorporated with the crude extracts successfully reduced the settlement of fouling organisms compared to the blank paint, as lesser macroalgae were found growing on the SL5%, DS5%, and DS10%. The LC-MS results showed 3-Methyloxiranyl phosphonic acid; (2RS,3SR)-form from the SL crude extract, while the 8-Decene-1,3,5-triol, 3-Hydroxyundecanoic acid, and 1-O-(6-Deoxy-6-sulfoglucopyranosyl)glycerol;  $\alpha$ -D-form, 3-Hexadecanoyl from the DS crude extract were involved in the antifouling properties. In conclusion, both crude extracts have the potential to be developed as antifouling agents.

**Keywords:** biofouling; marine resources; *Diadema setosum*; *Sonneratia lanceolata*; antifouling compounds



**Citation:** Mohd Ramzi, M.; Rahman, N.I.A.; Rawi, N.N.; Bhubalan, K.; Ariffin, F.; Mazlan, N.W.; Saidin, J.; Danish-Daniel, M.; Siong, J.Y.F.; Bakar, K.; et al. Antifouling Potential of *Diadema setosum* and *Sonneratia lanceolata* Extracts for Marine Applications. *J. Mar. Sci. Eng.* **2023**, *11*, 602. <https://doi.org/10.3390/jmse11030602>

Academic Editors: Gerardo Gold Bouchot, Azizur Rahman, Danqing Feng, Maria Salta and Chunfeng Ma

Received: 29 December 2022

Revised: 9 February 2023

Accepted: 9 March 2023

Published: 13 March 2023



**Copyright:** © 2023 by the authors. Licensee MDPI, Basel, Switzerland. This article is an open access article distributed under the terms and conditions of the Creative Commons Attribution (CC BY) license (<https://creativecommons.org/licenses/by/4.0/>).

## 1. Introduction

Biofouling is a process in which the accumulation of the undesired amount of marine organisms consisting of microfoulers (bacteria and protists) and macrofoulers (invertebrates and algae) is found on any submerged surfaces [1]. Biofouling has become a notable issue in maritime industries related to ship hulls (increased drag resistance), ship fuel systems (increment of water content in fuels), fuel and hydraulic systems (occlusion of sieves and valves), and in marine aquaculture (blockage of net and meshes) [1]. Marine industries have been spending a huge amount of money to manage and remove marine foulers on offshore facilities and other marine implements. The presence of marine organisms in the pipeline has been known to cause harmful effects on the performance of the pumps.

Fuel consumption amounts to 60% of the operation costs of a ship. However, after six months, the fuel consumption of a ship without antifouling paint increases by 40% due to the hull drag caused by high levels of fouling [2]. Antifouling in this situation refers to any strategic mechanism prohibiting the attachment of marine organisms to the manufactured surfaces [3]. Hence, coating the ship hull with antifouling paint could be the ultimate mechanism to minimize the impacts of foulers.

Antifouling paint was developed by incorporating biocides into the paints. For instance, toxic substances, such as copper or organotin compounds, have previously been the most beneficial method of controlling biofouling problems [4]. Although the biocides used were active ingredients to prevent biofilm formation, the majority of them were toxic and harmful to non-targeted organisms [5]. One of the commercial biocides used in antifouling paints for the past few years was tributyltin (TBT). However, the use of TBT caused environmental problems as it is detrimental to marine organisms. The marine application of TBT was banned by the International Maritime Organization and Marine Environment Protection Committee on 1 January 2008, due to an environmental concern [6]. The formulation of antifouling paints from natural resources is a different, more environmentally friendly way to address the biofouling issues that have arisen.

The incorporation of crude extracts of marine organisms that contain antifouling metabolites has been attempted by many researchers. A variety of marine natural products have been tested and were confirmed to have antifouling [7], antibacterial [8], antibiofilm [9], and antiprotozoan [10] properties. In addition, many marine organisms, as well as marine plants, have been reported to embrace the antifouling properties from seaweeds, soft corals, sponges, sea urchins, and mangrove species [11–13]. In a recent study, we targeted marine samples that have antifouling properties to minimize the biofouling problem. *Diadema setosum* (Leske, 1778) is one among six species of the *Diadema* genus and one of the widely distributed species within this genus [14]. *D. setosum* is a commodity traded in many countries and has a hard shell with five symmetrical shells inside. The shells of some *D. setosum* species are black-pigmented. In addition to hard shells, 95% of the pigment's body is dominated by fragile and toxic spines [15]. These spines are used for movement, defense, the stimulation of food, and certain types contain toxins [15]. The toxins from *D. setosum* can potentially be used in alternative antibiotic treatment [15]. Various studies have shown that *D. setosum* extracts have biological effects, such as antimicrobial [15,16], antifouling [12], and antioxidant [17] properties.

Mangrove species grow at the edge between the coastal and land area in subtropical and tropical regions of the world and are highly adapted to various temperatures, strong coastal winds, extreme tidal waves, salinity fluctuations, coastal water turbulence, river run-off, and anaerobic soil [18]. Most of these species are used as potential sources of biologically active chemicals that have commercial biotechnological applications and pharmaceuticals [19]. A number of mangroves and their associates contain poisonous substances, which also show biological activities such as antifungal, antibacterial, antifeedant, and pesticidal properties [20–23]. In addition, mangrove plants have been reported to possess steroids, triterpenes, saponins, flavonoids, alkaloids, and tannins [20,24,25]. *Sonneratia lanceolata* (Lythraceae) is a typical mangrove that is widely distributed from eastern Africa through Indo-Malaya to north-eastern Australia and some islands in the western Pacific Ocean [26,27]. However, limited studies have reported the biological effects of *S. lanceolata*, particularly in regard to their antifouling properties. Thus, in the current study, an attempt has been made to evaluate the antifouling activities of crude extracts of *D. setosum* and *S. lanceolata* against selected bacteria, as well as to develop antifouling paints incorporated with these crude extracts as antifoulant additives.

## 2. Materials and Methods

### 2.1. Samples Collections and Extractions

#### 2.1.1. *D. setosum*

Samples of *D. setosum* encoded as ECH1017001 (Figure 1A,B) were collected via scuba diving at Telok Belanga from the Archipelago of Pulau Bidong, Terengganu, Malaysia, which is located at 05°36.656' N 103°04.024' E. The *D. setosum* species was authenticated by Dr. Jasnizat Saidin from the Institute of Marine Biotechnology (IMB), Universiti Malaysia Terengganu (UMT), Malaysia. The *D. setosum* extraction was carried out according to the method described previously, with some modifications [12,28]. In the current study, the *D. setosum* was rinsed thoroughly with fresh water to detach the remaining surface salt. The fresh collected *D. setosum* was cleaned from any debris, chopped, and stored at −80 °C before lyophilization using a freeze dryer (Labconco, Kansas City, MO, USA). To obtain an ethanolic crude extract of *D. setosum*, 1510 g of the *D. setosum* powder was exhaustively macerated with 95% ethanol in a ratio of 1:10 (*w/v*). This procedure was repeated three times to maximize the extraction. After overnight maceration, the solution was filtered and evaporated using a vacuum rotary evaporator at 40 °C under reduced pressure to obtain ethanolic crude extract. This extraction yielded approximately 48.68 g of the dried crude extract of *D. setosum*, which was then stored at 4 °C until it use.

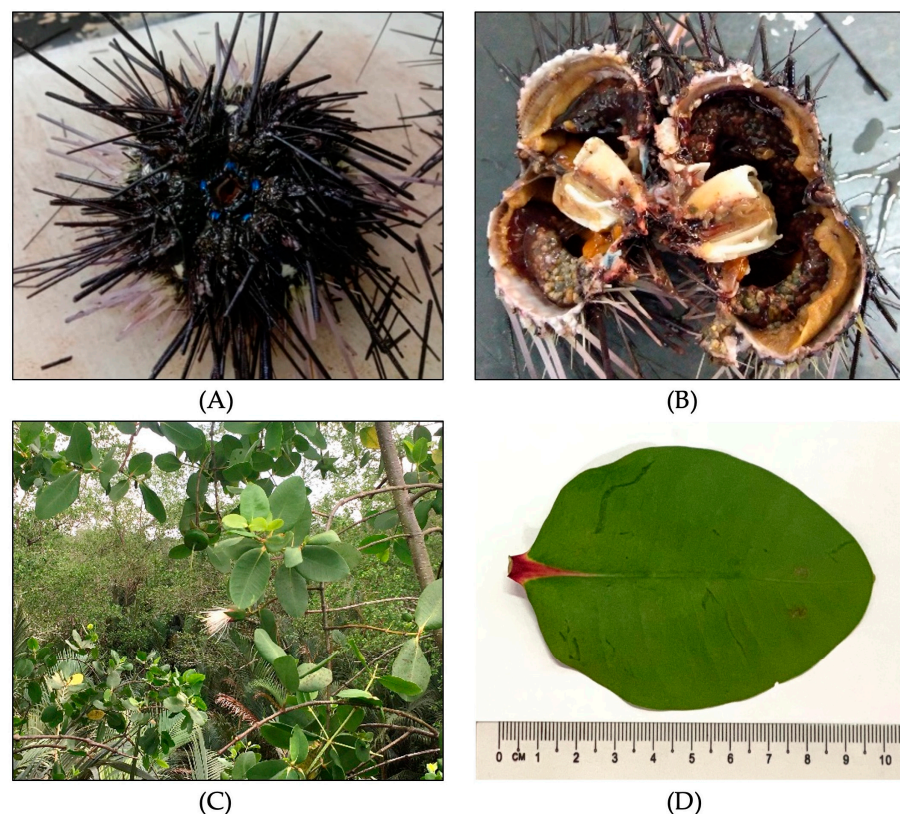


**Figure 1.** Morphology of the marine resources. (A) External structure of *D. setosum*, (B) Internal structure of *D. setosum*, (C) Leaves branches to end with flowers of *S. lanceolata*, (D) *S. lanceolata* leaves.

#### 2.1.2. *S. lanceolata*

Samples of *S. lanceolata* encoded as MAN0122001 (Figure 1C,D) were collected at an area in Universiti Malaysia Terengganu, 21030, Kuala Terengganu, Terengganu, Malaysia, which is located at 05°24'18.7' N 103°05'15.4' E. The mangrove plant species was authenticated by the field botanist, Haji Muhammad Razali Salam from the Faculty of Science and Marine Environment, Universiti Malaysia Terengganu, Terengganu, Malaysia. The extraction of the leaves from this mangrove plant was carried out according to the methods described by Andriani et al. [29] and Azemi et al. [30]. The *S. lanceolata* leaves were washed

and allowed to dry at room temperature for three days, then ground into a powder using an electric grinder. The powdered leaves (1580 g) were soaked in methanol at a ratio of 1:10 (*w/v*) overnight at room temperature. This procedure was repeated three times to maximize the extraction. The mixture was then filtered with Whatman No.1 filter paper (Merck, Darmstadt, Germany), and the filtrate was allowed to evaporate in a vacuum rotary evaporator (BUCHI, Flawil, Switzerland) set at 40 °C under reduced pressure. After the solvent was completely removed, the yield achieved was stored at 4 °C until use. In the current study, the extraction yielded 475.2 g of the paste-like crude extract of *S. lanceolata*.

## 2.2. Metabolomic Technique

The dereplication study on the total crude extract of the samples was performed using HRESI-LCMS and processed with the MZmine 2.40.1 software [31], an in-house macro coupled with the Dictionary of Natural Products (DNP) 2017 and SIMCA P+ 15 (Umetrics AB, Umeå, Sweden). The mass spectral data were processed using the procedure by MacIntyre et al. [32], which was established in the Natural Products Metabolomics Group Laboratory at SIPBS, University of Strathclyde, Glasgow, UK, as described previously [32,33].

## 2.3. Dereplication by Using HRESI-LCMS

The procedure and program for HRESI-LCMS were set up as described below. Each extract of 1 mg/mL in methanol was analyzed on an Accela HPLC (Thermo Fisher Scientific, Waltham, MA, USA) coupled with a UV detector at 280 and 360 nm and an Exactive-Orbitrap high-resolution mass spectrometer (Thermo Fisher Scientific, MA, USA). A methanol blank was also analyzed. The column attached to the HPLC was a HiChrom, ACE (Berkshire, UK) C<sub>18</sub>, 75 mm × 3.0 mm, 5 μm column. The mobile phase consisted of micropore water (A) and acetonitrile (B) with 0.1% formic acid for each solvent. The gradient program started with 10% B and linearly increased to 100% B within 30 min at a flow rate of 300 μL/min, and remained isocratic for 5 min before linearly decreasing back to 10% B in 1 min. The column was then re-equilibrated with 10% B for 9 min before the next injection. The total analysis time for each sample was 45 min. The injection volume was 10 μL and the tray temperature was maintained at 12 °C. High-resolution mass spectrometry was carried out in both the positive and negative ESI ionization switch modes, with a spray voltage of 4.5 kV and capillary temperature at 320 °C. The mass range was set between *m/z* 150–1500 for the ESI-MS range.

The mass spectral data were processed using the procedure by MacIntyre et al. [32], which was established in the Natural Products Metabolomics Group Laboratory at SIPBS, as described previously [32,33]. The LC-MS chromatograms and spectra were viewed using Thermo Xcalibur 2.1 (Thermo Fisher Scientific, MA, USA) or MZmine 2.40.1. The raw data were initially sliced into negative and positive data sets using the MassConvert software package from ProteoWizard (3155 Porter Drive, Palo Alto, CA, USA). The sliced data sets were subsequently exported into MZmine 2.40.1. The spectra were crop-filtered from 4 min to 40 min. The peaks in the samples and solvent and media blanks (where applicable) were detected using the chromatogram builder. The mass ion peaks were isolated using a centroid detector threshold that is greater than the noise level, set at  $1.0 \times 10^4$  using an MS level of 1. The chromatogram builder was used with a minimum period set at 0.2 min, and the minimum height and *m/z* tolerance at  $1.0 \times 10^4$  and 0.001 *m/z* or 5.0 ppm, respectively. Chromatogram deconvolution was then performed to detect the individual peaks. The local minimum search algorithm (chromatographic threshold: 90%, search minimum in retention time (Rt) range: 0.4 min, minimum relative height: 5%, minimum absolute height:  $3.0 \times 10^4$ , the minimum ratio of peak top/edge: 2, and peak duration range: 0.3–5 min) was applied. Isotopes were also identified using the isotopic peaks grouper (*m/z* tolerance: 0.001 *m/z* or 5.0 ppm, Rt tolerance: 0.2 absolute (min), maximum charge: 2, and representative isotope: most intense). The Rt normalizer (*m/z* tolerance: 0.001 *m/z* or 5.0 ppm, Rt tolerance: 5.0 absolute (min)), and minimum standard intensity: ( $5.0 \times 10^3$ ) were used to reduce the inter-batch variation. The peak lists were all aligned using the

join aligner parameters set at  $m/z$  tolerance: 0.001  $m/z$  or 5.0 ppm, weight for  $m/z$ : 20, Rt tolerance: 5.0 relative (%), and weight for Rt: 20. Missing peaks were detected using the gap-filling peak finder (intensity tolerance: 1.0%,  $m/z$  tolerance: 0.001  $m/z$  or 5.0 ppm, and Rt tolerance of 0.5 absolute (min)). An adduct search was performed for both the negative and positive modes. For the ESI negative mode, formate adducts were searched for (Rt tolerance: 0.2 absolute (min),  $m/z$  tolerance: 0.001  $m/z$  or 5.0 ppm, max relative adduct peak height: 30%). A complex search was also performed with the ionization method  $[M - H]^-$ . For the ESI-positive mode, the adducts that were searched included Na+H, K+H, NH<sub>4</sub>, and ACN+H. A 5.0 absolute (min), and a minimum standard intensity: ( $5.0 \times 10^3$ ) were used to reduce the inter-batch variation. The peak lists were all aligned using the join aligner parameters set at  $m/z$  tolerance: 0.001  $m/z$  or 5.0 ppm, weight for  $m/z$ : 20, Rt tolerance: 5.0 relative (%), and weight for Rt: 20. Missing peaks were detected using the gap-filling peak finder (intensity tolerance: 1.0%,  $m/z$  tolerance: 0.001  $m/z$  or 5.0 ppm, and Rt tolerance of 0.5 absolute (min)).

The processed data set was then subjected to molecular formula prediction and peak identification. The data sets were exported to CSV (comma delimited) to be imported to the in-house macro workstation. By using the macro, both the negative and positive data sets were imported for preparation, followed by the removal of all the media blanks and the samples. The macro combined all of the processed data from the different media and samples and then prepared for the final data set to be imported to SIMCA P+ 15, followed by the dereplication step using the AntiMarin and DNP databases. The combined data set was imported into SIMCA P+ 15 for multivariate analysis. Pareto scaling was applied. Principle Component Analysis (PCA) and supervised Orthogonal Projections to Latent Structures Discriminant Analysis (OPLS-DA) were used to compare the metabolic profiles of the different samples and to evaluate their unique secondary metabolites. The models were validated by a permutation test. The Y-intercept ( $Q^2Y$ ) on the permutation graph is a measure to check against overfitting. A clear indication that the model is valid and does not happen by coincidence is when the  $Q^2$  values of the permuted Y models are less than zero on the permutation plot test. Moreover, the difference between  $Q^2$  and  $R^2Y$  must be less than 0.3, indicating the absence of overfitting.

#### 2.4. Preparation of Panels Incorporated with *D. setosum* and *S. lanceolata* Crude Extracts

The panels used in this study were painted steel panels received from a local Oil and Gas company (Bandar Baru Bangi, Selangor, Malaysia). The panels were cut into square shapes with dimensions of 2.5 cm  $\times$  2.5 cm  $\times$  0.3 cm (Figure 2A). The paint on the panels was removed by hand tool cleaning, equipped with a sanding machine following the SSPC-SP2 standard. The steel panels were polished using rough-grade abrasive paper fixed to an orbital sander to remove the rust before proceeding with the coating method. Then, according to the SSPC-SP1 standard, the panels were cleaned using methanol to remove all detectable oil, grease, dust, or other soluble contaminants [34]. Furthermore, the cleaning process is required to provide good adhesion between the primer and the metallic substrate.

Blank paint with no antifouling agent and commercial antifouling paint, known as reference paint 1 (RF1) and 2 (RF2), received from the industry (provided by a local Oil and Gas company) were used for this study, which act as the negative and positive controls, respectively. Blank paint is a mixture of paint consisting of some chemicals, including: colophony (CAS number: 8050-09-7), xylene (CAS number: 1330-20-7), zinc oxide (CAS number: 1314-13-2), ethylbenzene (CAS number: 100-41-4), hydrocarbons (C9, aromatic, CAS number: 64742-95-6), 1-methoxy-2-propanol (CAS number: 107-98-2), and fatty acids (CAS number: 91001-64-8). Some of the components included in the reference paints are similar to the blank paint, but without fatty acids and other ingredients added. In addition, the other ingredients contained in the reference paints were dicopper oxide (CAS number: 1317-39-1), and zineb (CAS number: 12122-67-7). According to Salama [35], the selected weights of the crude extracts were diluted with a small amount of solvent to dissolve the

extracts. Commercial thinners that contained a mixture of xylene (CAS number: 1330-20-7) and ethylbenzene (CAS number: 100-41-4) were used as a solvent in this experiment to dilute the extracts and control the viscosity of the paint. The crude extracts of *D. setosum* (DS) and *S. lanceolata* (SL) were incorporated into the blank paint to obtain the final concentration of mixed paint, which were 5% (DS5% and SL5%) and 10% (DS10% and SL10%) weight per volume. Then, the mixtures were mixed using a drilling machine to form a homogeneous antifouling paint. The steel panels contained three replicate panels ( $n = 3$ ) that were painted with an air spray compressor (Model ZL-550W×2-50L, Uma, Cheras, Selangor, Malaysia) and allowed to dry for 2 days between each coating. Three layers of paint were applied, and the first coating was the commercial anticorrosive primer, with three times coating to obtain a final dry film thickness of  $150 \pm 5 \mu\text{m}$  followed by the antifouling paint and commercial antifouling paint with two times coating to obtain  $100 \pm 5 \mu\text{m}$ . The Dry Film Thickness (DFT) is the thickness of the coating materials measured on the above surfaces. In this study, the DFT of the steel panels was measured at five different sides for each panel using a digital coating thickness gauge, PosiTector 6000 (Ogdensburg, NY, USA).

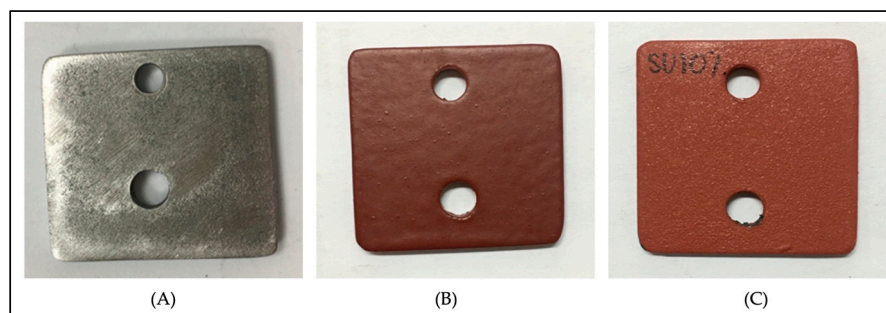


**Figure 2.** Preparation of panels. (A) Uncoated panel. (B) Panel coated with anticorrosive primer. (C) Panel coated with anticorrosive primer and antifouling extract (*D. setosum* or *S. lanceolata*).

## 2.5. Antibiofilm Assays in the Laboratory

### 2.5.1. Crystal Violet Assay

An antifouling crystal violet assay was performed according to the method previously described by Idora et al. [34]. This method was applied to study the antifouling properties of the crude extracts towards biofilm-producing bacteria *Pseudomonas aeruginosa* (*P. aeruginosa*). Next, 100  $\mu\text{L}$  of each sample with a concentration of 10 mg/mL was loaded into a 96-well microtiter plate and left enclosed with the lid. After an hour, 100  $\mu\text{L}$  of the bacterial suspension was inoculated into the well of the sample. The wells loaded only with the bacterial suspension were assigned as the negative control. The biofilm was allowed to develop for 24 h while being aerobically incubated at 37 °C. The plate was decanted, washed, and set to dry prior to 20 min of staining with 200  $\mu\text{L}$  of 1% crystal violet at room temperature. Then, 200  $\mu\text{L}$  of distilled water was used to rinse out the excess stain, and this was repeated three times. After 15 min of air-dry, 200  $\mu\text{L}$  of 30% acetic acid as the solubilizer of the well-bound stain was pipetted and incubated for 10 min at room temperature. The plate was agitated and measured at OD<sub>595</sub> using a Multiskan Skyhigh Microplate Spectrophotometer (Thermo Fisher Scientific, MA, USA). The percentage of the biofilm reduction was calculated following the methods described by Leroy et al. [36]

### 2.5.2. Biofilm Formation Test in Aquarium

All of the panels were pendent in an aquarium tank containing 141 L of fresh seawater and the tank was kept at room temperature with a waves mimicking condition. A total of 1.41 L of sterile artificial seawater [37] (Table 1) was added to the seawater to provide the essential nutrients. The panels were retrieved from the aquarium tank after 24 h. The biofilm attached to the panels (control and antifouling paint) was scraped off using a cotton swab and suspended in 1 mL of sterile artificial seawater. This suspension was subjected to serial dilution and was spread on Zobell marine agar (ZMA) plates. Then, the agar

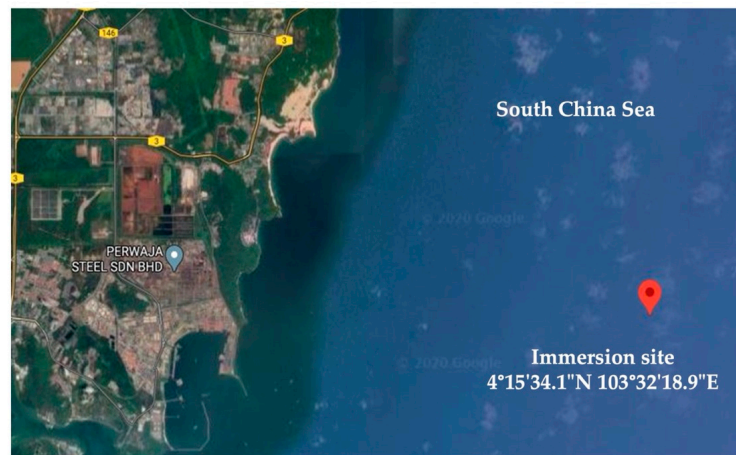
plates were kept in the incubator at a temperature of 37 °C for the development of bacterial colonies. Twenty-four hours later, the growing colonies were computed by using a microbial colony counter (LAPIZ, Medica) [38]. All the panels were prepared with triplicates.

**Table 1.** Composition of artificial seawater.

Ingredients	Quantity (g/L)
NaCl	24.615
KCl	0.783
Na <sub>2</sub> SO <sub>4</sub>	4.105
MgCl <sub>2</sub> (H <sub>2</sub> O) <sub>6</sub>	11.06
CaCl <sub>2</sub> (H <sub>2</sub> O) <sub>2</sub>	1.558

**2.6. Antimicrofouling Activity of Painted Panels in Field Assay**

The coated steel panels were immersed in seawater at Kemaman and Pulau Redang. The panels were deployed on 17 September 2020 for Kemaman and 25 September 2020 for Pulau Redang (Figure 3A,B, respectively). The experiment was carried out by submerging the panels, which were attached to a stainless steel frame (Figure 4), for five weeks at both sites and were deposited 2 m from the bottom of the ocean. The depth of water at Kemaman was 27 m and 17 m for Pulau Redang. The panels were retrieved weekly by diving and brought back to the laboratory for further analysis. The physical parameters of the surrounding seawater were recorded using a hand-held multimeter (Aquaread Asia, Singapore).



(A)



(B)

**Figure 3.** The sampling sites where the panels were submerged underwater; are (A) Kemaman, and (B) Pulau Redang. <https://www.google.com/maps/@5.3873277,103.0933283,15z>, accessed on 6 May 2021.

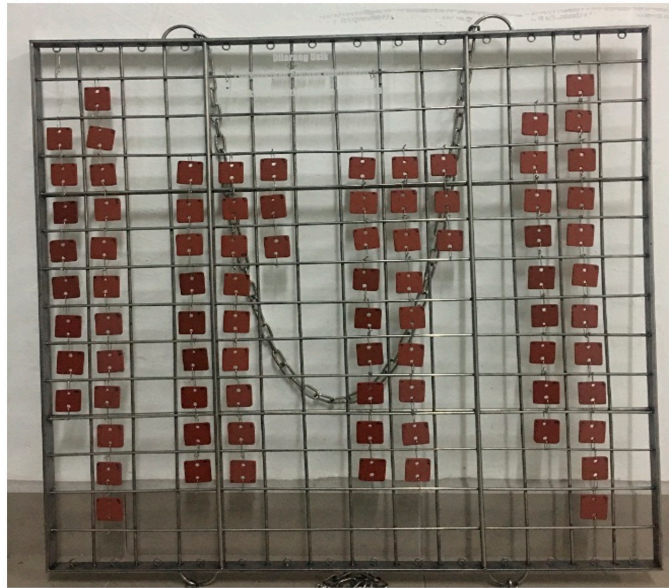


**Figure 4.** Stainless steel frame with coated steel panels for testing.

### 2.7. Statistical Analysis

The data were expressed as mean  $\pm$  standard error of the mean (SEM). Statistical analysis of the data was performed using the GraphPad Prism software version 8.0 (GraphPad Software, San Diego, CA, USA). Differences between the groups were analyzed using a one-way analysis of variance (ANOVA) followed by Turkey's post hoc test. Statistical significance was defined when the  $p$ -value was less than 0.05 ( $p < 0.05$ ).

## 3. Results and Discussion

### 3.1. Dereplication Studies of *D. setosum* and *S. lanceolata* Extract

The dereplication study of the extracts of *D. setosum* and *S. lanceolata* was performed using the HREI-LCMS data. Based on the antifouling activity and the amount of the extracts, further investigation of the metabolites on the extracts of *D. setosum* and *S. lanceolata* was carried out. An OPLS-DA model was used to investigate the variation and diversity of the various extracts. The unique metabolites at the end of the S-loadings plot in the active extract of *D. setosum* were indicated by Rt at 3.20 min ( $[M + H]^+$  ion peaks at  $m/z$  189.149) and 5.17 min ( $[M + H]^+$  ion peaks at  $m/z$  203.164), indicating antifouling activity, which gave a match from the database, namely 8-Decene-1,3,5-triol and 3-Hydroxyundecanoic acid, respectively (Figure 5). Meanwhile, the ion at Rt at 22.0 min (Figure 5) revealed that this metabolite matched with the molecular formula  $C_{25}H_{48}O_{11}S$ , which was putatively identified as 1-*O*-(6-Deoxy-6-sulfoglucopyranosyl)glycerol;  $\alpha$ -D-form, 3-Hexadecanoyl from sea urchin *Anthocardaris crassispina* [39], the brown algae *Sargassum thunbergii* [40,41] and *S. wightii* [42] and the red algae *Caulacanthus ustulatus* [41]. The total ion chromatogram of the extract *D. setosum* (Figure 5) showed the distribution of the obtained secondary metabolites (Supplementary Table S1). A few predicted metabolites from the sea urchin species matched the database, including at Rt 2.24, 7.72, and 25.57 min (Supplementary Table S1), which were from the eggs of the sea urchin, *Echinocardium cordatum* and *Strongylocentrotus purpuratus*, respectively. Meanwhile, the metabolites predicted at Rt 18.33, 28.68, and 31.96 min (Supplementary Table S1) were identified from *Anthocardaris crassispina*, *Tripneustes esculentus*, and *Anthocardaris crassispina*.



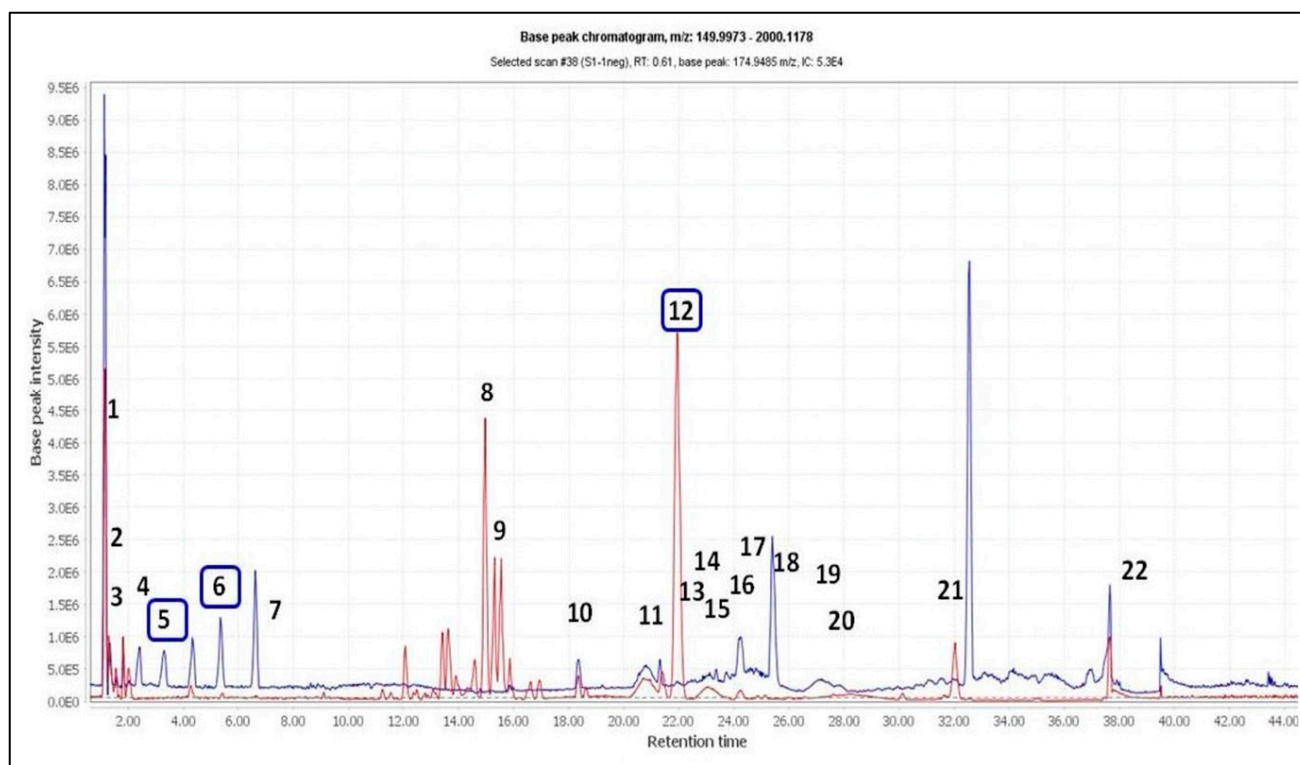
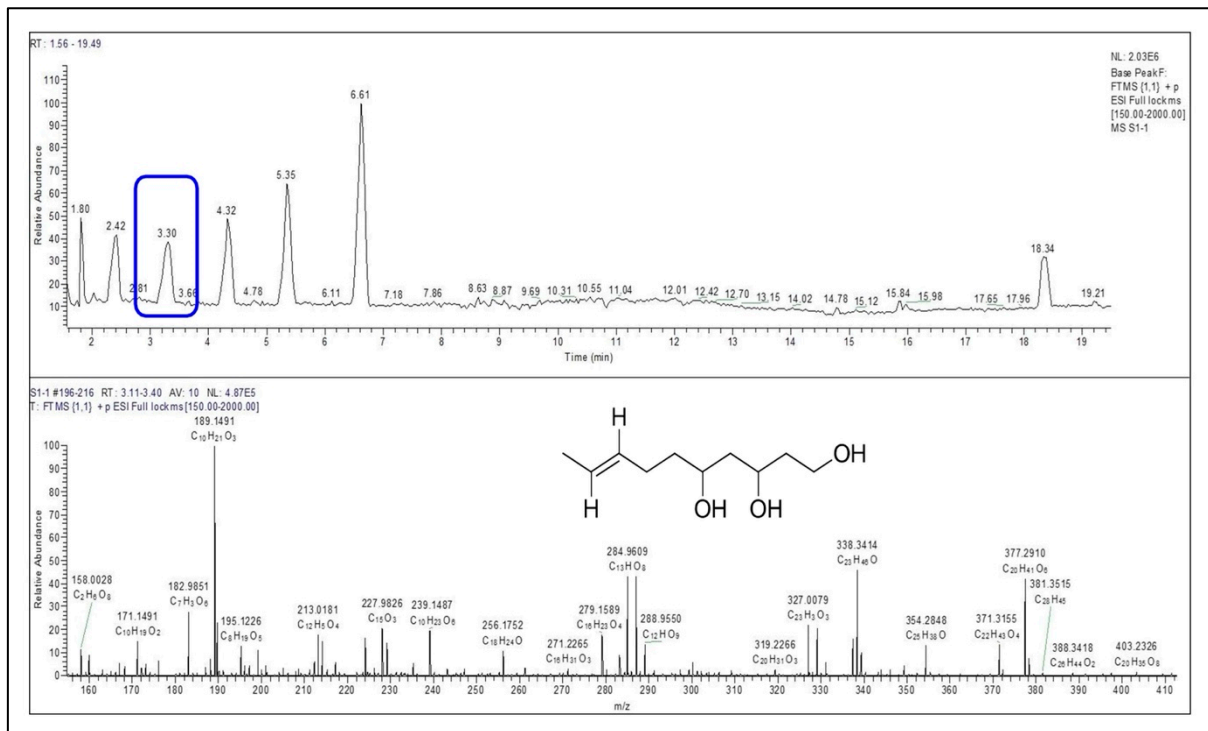
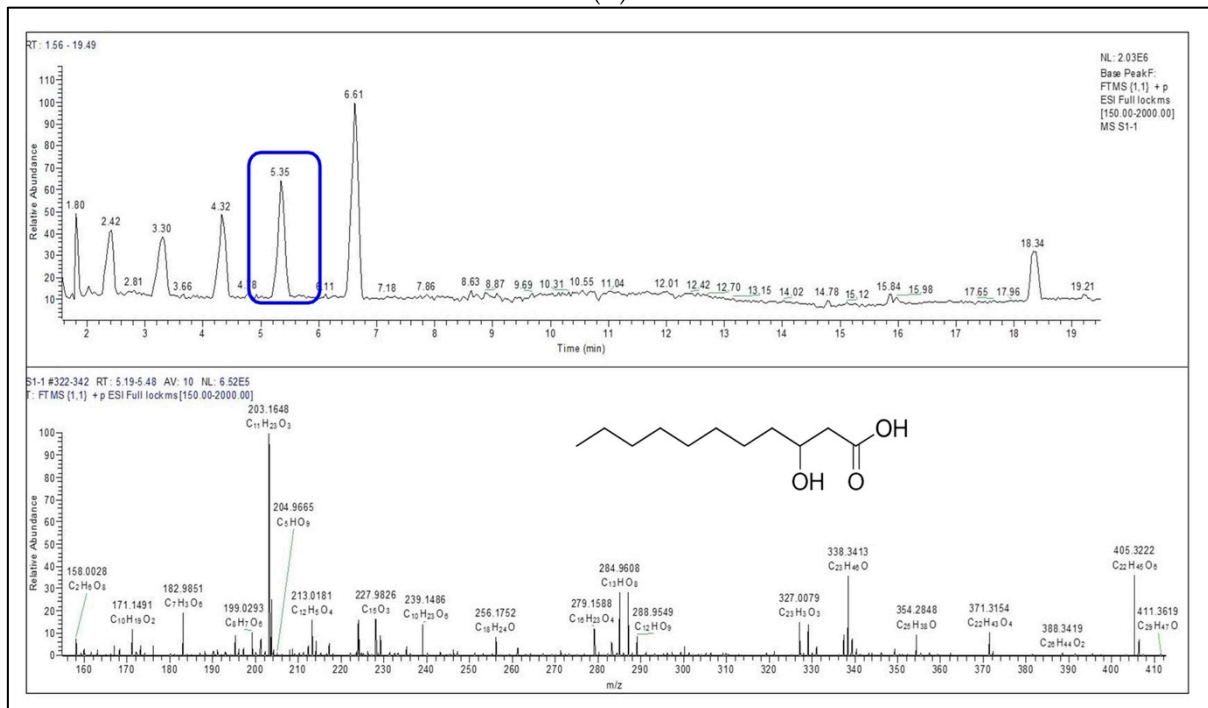


**Figure 5.** Total ion chromatogram (TIC) of the extract of *D. setosum* (blue and red represent positive and negative ionization modes, respectively). The dereplication of numbered peaks is shown in Supplementary Table S1. E0:  $1.0 \times 10^0$ ; E5:  $1.0 \times 10^5$ ; E6:  $1.0 \times 10^6$ .

The metabolites indicated at Rt 3.30 min ( $m/z$ : 189.1489; Figure 6A) and 5.35 min ( $m/z$ : 203.1648; Figure 6B) are putatively identified as fatty acids that are potent for antifouling activity [43]. The previous study reported that the fatty acid groups were potent for antifouling activity, including 1-Hydroxymyristic acid and 9-Z-oleic acid isolated from the marine bacteria *Shewanella oneidensis* and 12-Methylmyristic isolated from *Streptomyces* sp. [44]. Meanwhile, the ion peak contributed to a compound containing sulfur at Rt 21.94 min ( $[M - H]^-$  at  $m/z$  555.2846) from the extract of *D. setosum* that is responsible for antifouling activity (Figure 6C). A study by Fusetani [45] has reported that the mixture of compounds 1:1 between flouridoside possessing a glucoside ring and isethionic acid containing sulfur were potent in a larval settlement inducer, but not as an individual compound [45]. Recently, a study on phenolic acid containing glucoside and sulfur reported that rutin persulfate, 3,6-bis( $\beta$ -D-glucopyranosyl) xanthone persulfate and gallic acid persulfate showed potent anti-settlement activity and were non-toxic [46]. Dahms and Dobretsov [1] have shown that 2-(dodecanoyloxy)ethane-1-sulfonate with the presence of a sulfonyl group showed very promising antifouling activity. A study by Petitbois [47] reported that methyl (Z)-octadec-11-enoate and methyl (5Z,9Z)-hexacos-5,9-dienoate possessing one and two unsaturated double bonds, respectively, gave potent antifouling activity.

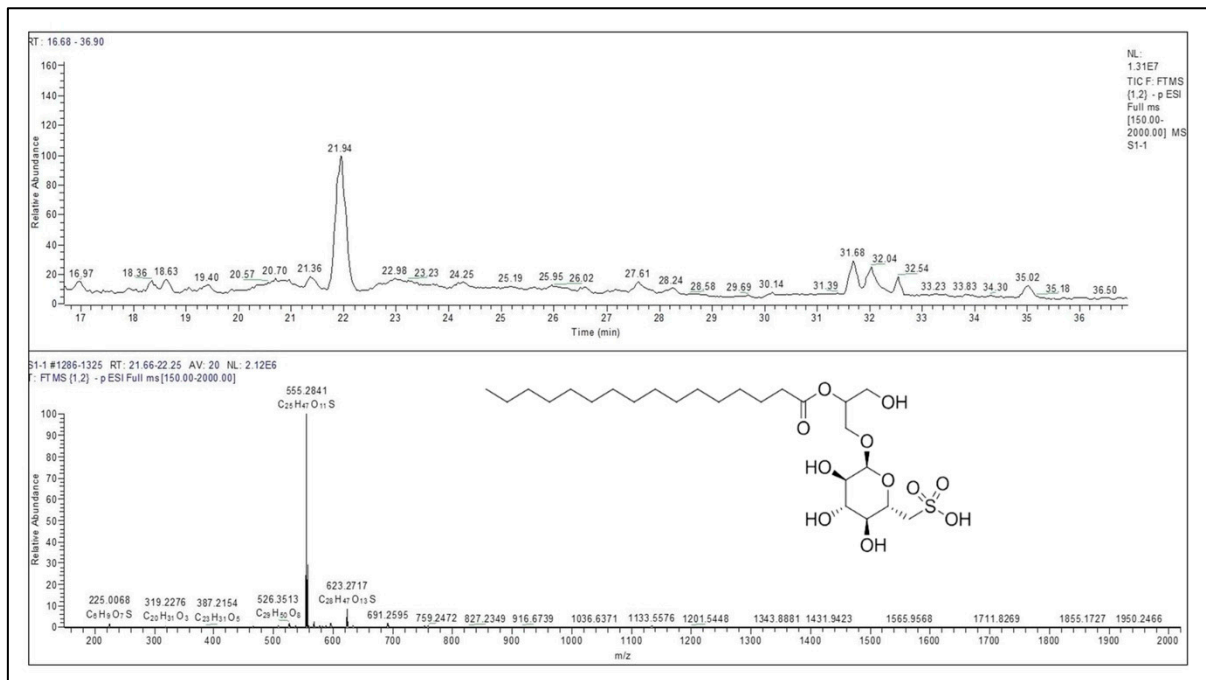


(A)



(B)

Figure 6. Cont.



(C)

**Figure 6.** Total ion chromatogram of the *D. setosum* extract of an ion peak at  $m/z$ . (A) 189.1492  $[M + H]^+$  matched the molecular formula  $C_{10}H_{20}O_3$ , putatively identified as 8-Decene-1,3,5-triol, (B) 203.1648  $[M + H]^+$  matched the molecular formula  $C_{11}H_{22}O_3$ , putatively identified as 3-Hydroxyundecanoic acid and (C) 556.2841  $[M + H]^+$  matched the molecular formula  $C_{25}H_{48}O_{11}S$ , putatively identified as 1-O-(6-Deoxy-6-sulfolglucopyranosyl) glycerol;  $\alpha$ -D-form, 3-Hexadecanoyl. RT: retention time; E0:  $1.0 \times 10^0$ ; E5:  $1.0 \times 10^5$ ; E6:  $1.0 \times 10^6$ ; E7:  $1.0 \times 10^7$ .

An OPLS-DA model was used to investigate the variation and diversity of the *S. lanceolata* extract. The total ion chromatogram of the extract *S. lanceolata* (Figure 7) showed the distribution of the obtained secondary metabolites (Supplementary Table S2). Previous studies have reported that metabolites, particularly astragalin, antirrhinoside, and scopine, demonstrated anti-bacterial properties [48–50]. These metabolites were matches with the astragalin ( $C_{21}H_{20}O_{11}$ ), antirrhinoside; 5-Epimer, 6'-O-(4-hydroxy-Z-cinnamoyl)( $C_{24}H_{28}O_{12}$ ), and scopine ( $C_{10}H_{15}NO_3$ ) isolated from *S. lanceolata* at Rt 7.71, 8.66, and 25.37 min (Supplementary Table S2), respectively, via HREI-LCMS. The peak ID 2 at Rt 1.31 min ( $m/z$ : 217.0630; Figure 8) gave a match from the database with a molecular formula  $C_9H_{15}O_4P$ , putatively identified as 3-Methyloxiranyl phosphonic acid; (2R,3S)-form, Di-2-propenyl ester, also known as Fosfomycin. This metabolite was also isolated from *Streptomyces fradiae* [51–53].

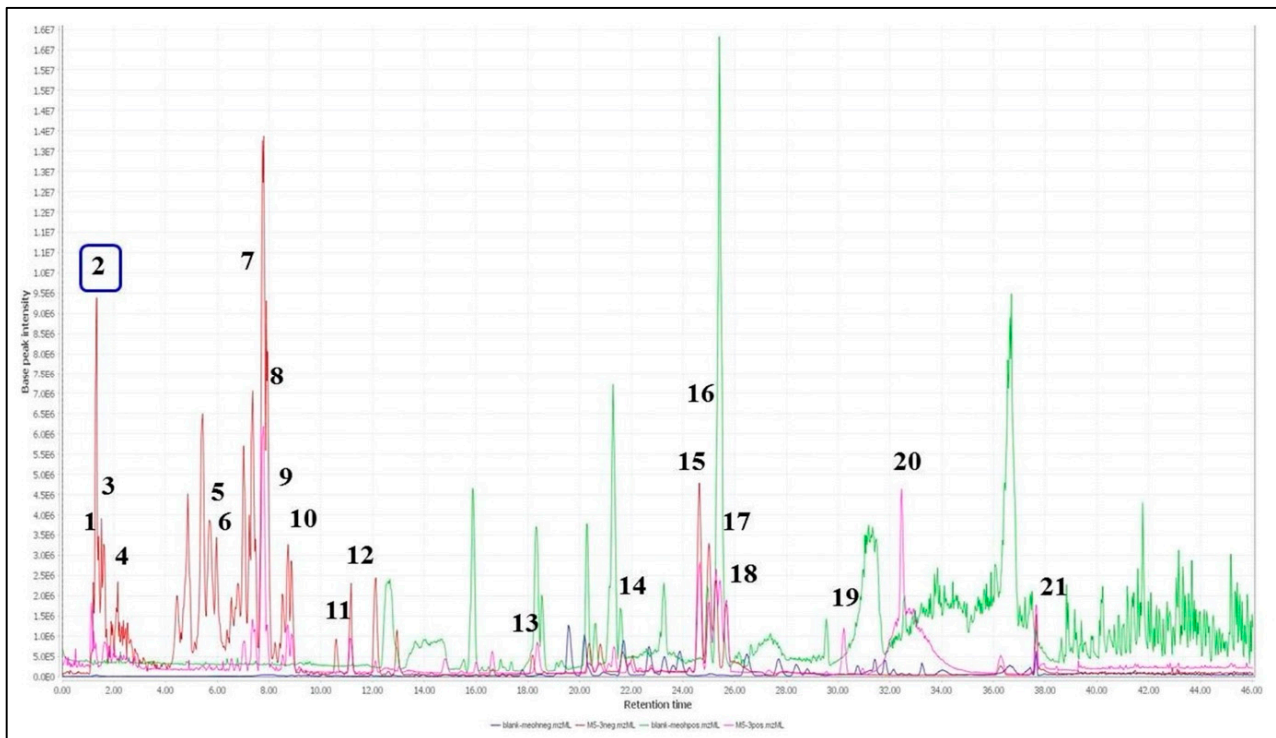


**Figure 7.** Total ion chromatogram of the extract of *S. lanceolata* (red and violet represent positive and negative ionization modes, respectively). Green and black peaks represent the methanol used in this analysis that acts as blank. The dereplication of numbered peaks is shown in Supplementary Table S2. E0:  $1.0 \times 10^0$ ; E5:  $1.0 \times 10^5$ ; E6:  $1.0 \times 10^6$ ; E7:  $1.0 \times 10^7$ .

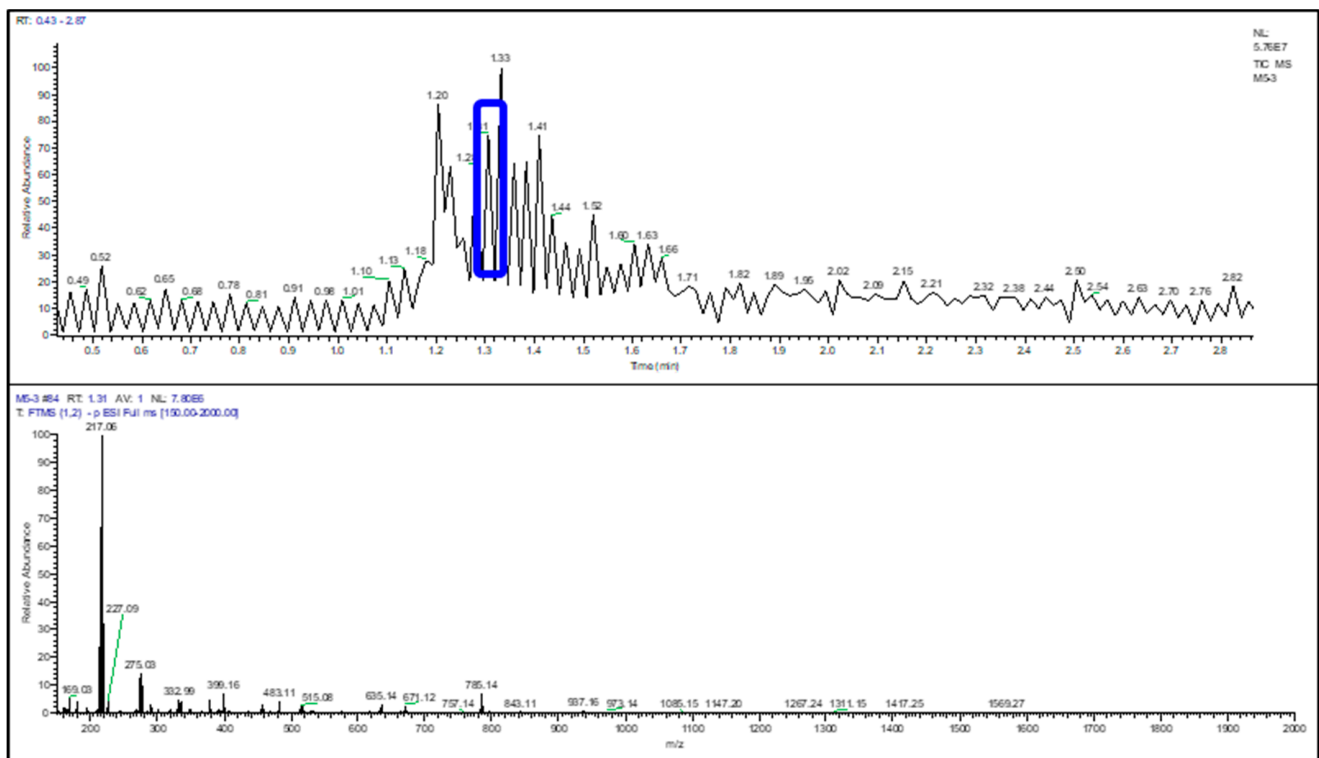


**Figure 8.** Total ion chromatogram of the *S. lanceolata* extract of an ion peak at  $m/z$  217.0630  $[M + H]^+$  matched the molecular formula  $C_9H_{15}O_4P$ , putatively identified as (3-Methyloxiranyl)phosphonic acid; (2RS,3SR)-form, Di-2-propenyl ester. E6:  $1.0 \times 10^6$ ; E7:  $1.0 \times 10^7$ .

### 3.2. Painted Panels with Crude Extract

Table 2 shows the average Dry Film Thickness (DFT) of the panels after coating with the primer (1st coating) and antifouling paints (2nd coating) measurement. The DFT results for the anti-corrosive primer and the antifouling paint extract were  $151.30 \pm 6.40 \mu\text{m}$  and  $253.80 \pm 7.79 \mu\text{m}$ , respectively (Table 2). It is indicated that the DFT of all these panels was similar and can be used for this experiment.

**Table 2.** Average DFT of the panels after coating with primer (1<sup>st</sup> coating) and painted panels with crude extracts (2nd coating).

1st Coating (Panels Coated with Anti-Corrosive Primer)	Dry Film Thickness ( $\mu\text{m}$ )	Average ( $\mu\text{m}$ )
Panel 1	156.00	$151.30 \pm 6.40$
Panel 2	151.00	
Panel 3	160.00	
Panel 4	148.00	
Panel 5	150.00	
Panel 6	161.00	
Panel 7	143.00	
Panel 8	153.00	
Panel 9	149.00	
Panel 10	142.00	
2nd Coating (Blank Paint and Painted Panels with Crude Extracts)	Dry Film Thickness ( $\mu\text{m}$ )	Average ( $\mu\text{m}$ )
Panel 1	262.00	$253.80 \pm 7.79$
Panel 2	243.00	
Panel 3	250.00	
Panel 4	257.00	
Panel 5	265.00	
Panel 6	240.00	
Panel 7	253.00	
Panel 8	257.00	
Panel 9	254.00	
Panel 10	257.00	

### 3.3. Antibiofilm Assay in the Laboratory

#### 3.3.1. Crystal Violet Assay

The present crude extracts of *D. setosum* and *S. lanceolata* were shown to have antifouling properties, with different levels of effectiveness at different concentrations. This effect of both the crude extracts was shown by the high percentage inhibition of the *P. aeruginosa* biofilm (Figure 9). However, no significant differences were seen between *D. setosum* and *S. lanceolata* at different concentrations. In addition, at the lowest concentration of both the crude extracts (0.6125 mg/mL), it was shown that the effects of the lowest concentration have a comparable effect with the highest concentration (10.00 mg/mL) in biofilm inhibition (no significant difference between the concentrations,  $p > 0.05$ ). It has been shown that both the crude extracts were effective at the lowest concentration against the *P. aeruginosa* biofilm.

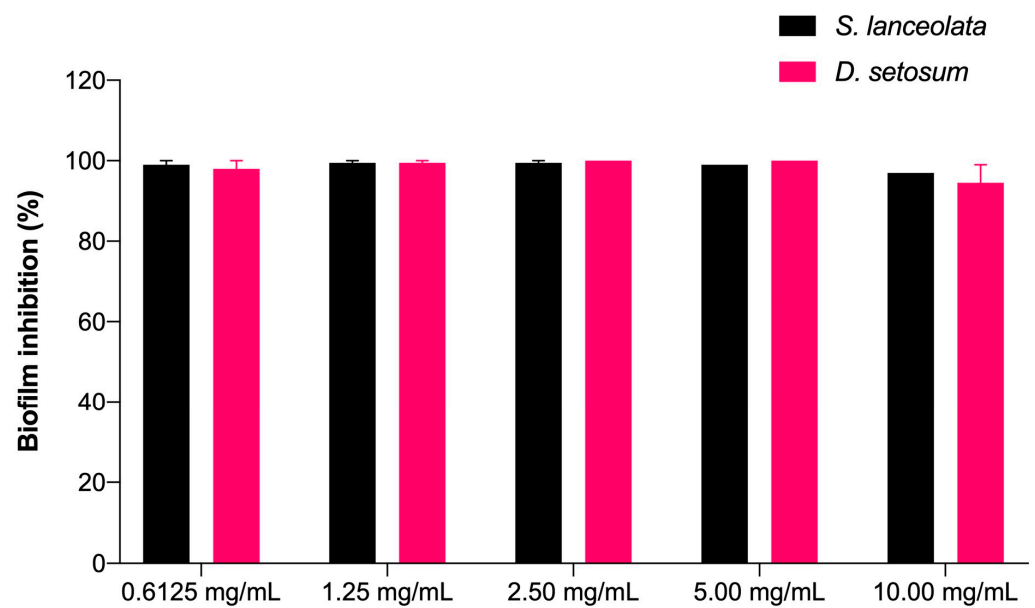


**Figure 9.** The percentage of *P. aeruginosa* biofilm inhibited by *D. setosum* and *S. lanceolata* crude extract with respect to concentration in antifouling assay. Data were presented as mean  $\pm$  SEM ( $n = 3$ ).

### 3.3.2. Biofilm Formation Test in Aquarium

In the current study, the formation of biofilms on the coated panels was tested in an aquarium setup. The biofilm attachment was determined by measuring the bacterial counts from the biofilms attached. It was found that the antifouling paint incorporated with an antifouling agent from the crude extracts reduced the settlement of marine bacteria compared to the blank paint (negative control).

The number of bacterial cells attached to the panels coated with blank paint, which acted as the negative control, was found to be  $700.1 \times 10^3$  CFU/mL, while it was significantly reduced to  $296.9 \times 10^3$  CFU/mL ( $p < 0.01$ ) on the panels coated with antifouling paint (DS10%) and  $343.6 \times 10^3$  CFU/mL ( $p < 0.01$ ) on the agar plate spread with the bacterial suspension from the panels coated with SL 10%. Similarly, the number of bacterial cells attached to the panels coated with the antifouling paints, which are from the DS5% and SL5%, significantly reduced the biofilm attachment of bacteria, found to be  $183.5 \times 10^3$  CFU/mL ( $p < 0.001$ ) and  $111.3 \times 10^3$  CFU/mL ( $p < 0.001$ ), respectively (Figure 10). In another study, an antifouling coating made by incorporating the crude extract of Palmyra palm (*Borassus flabellifer*) into epoxy resin significantly reduced the adhesion of biofilm bacteria in an in vitro experiment and macrofoulers in the field study [54]. Similarly, the current study's findings showed that antifouling paint incorporated with the crude extracts of *D. setosum* and *S. lanceolata* can inhibit the settlement of bacteria from adhering to the surfaces in laboratory conditions.

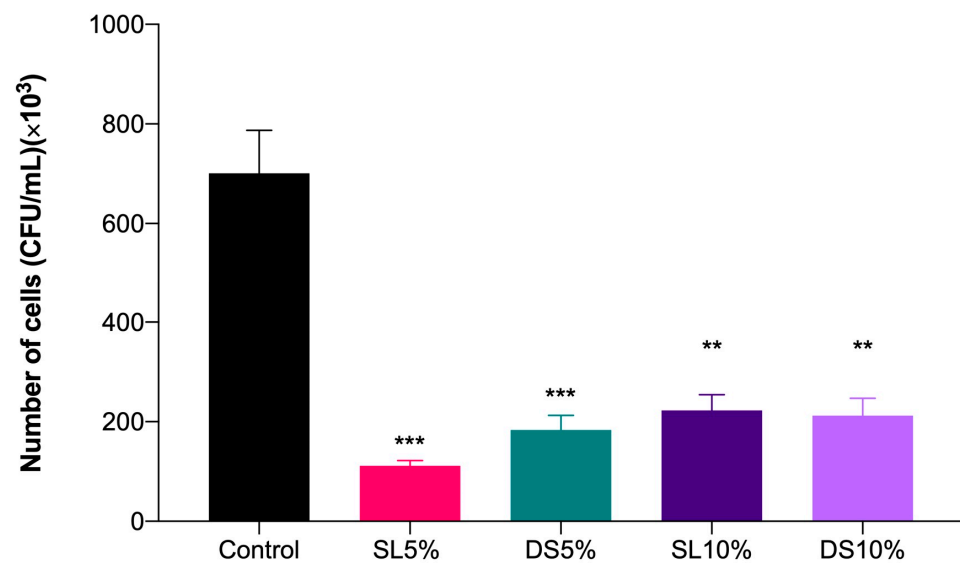
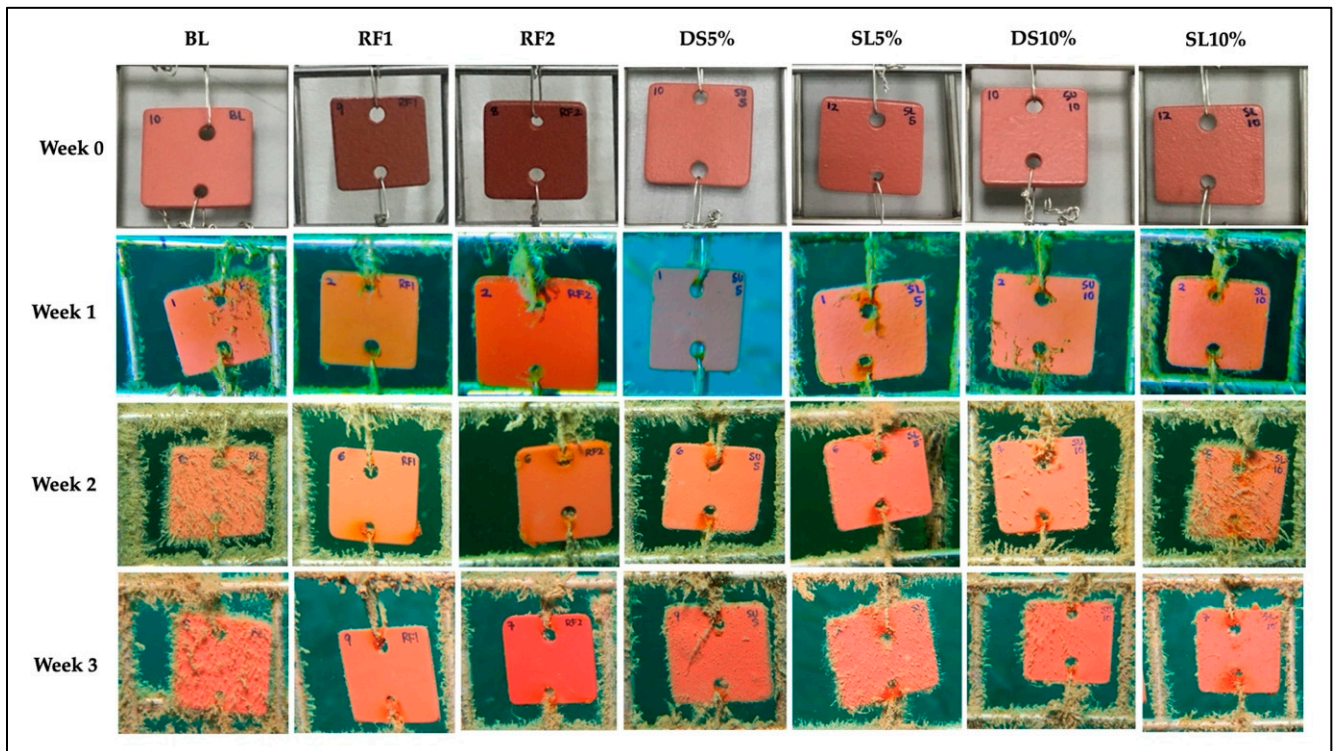


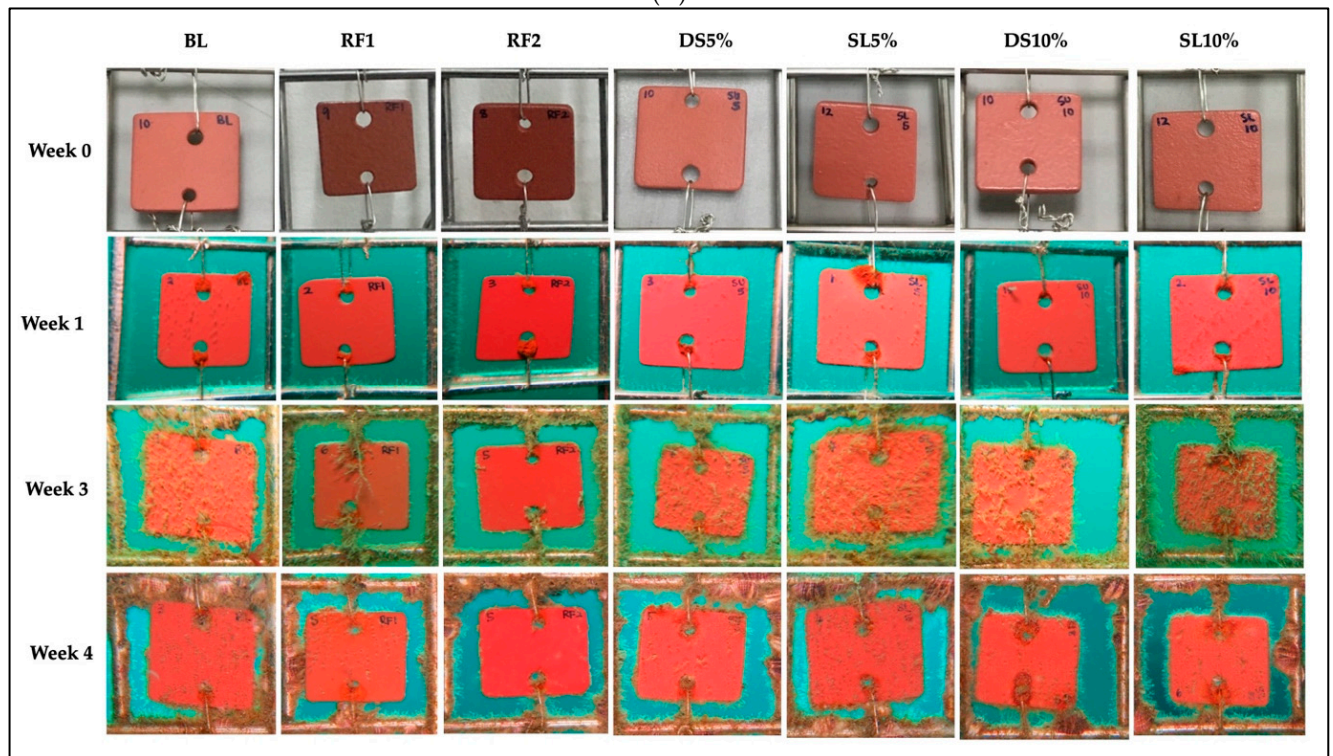
**Figure 10.** Bacterial count (CFU/mL) for the tested panels in an aquarium after 24 h of incubation. Data are presented as mean  $\pm$  SEM ( $n = 3$ ). \*\*  $p < 0.01$ , \*\*\*  $p < 0.001$  vs. Control.

### 3.4. Antimacrofouling Activity of Painted Panels in Field Assay

The crude extracts of *D. setosum* and *S. lanceolata* were used with two different concentrations: 10% (DS10% and SL10%), and 5% (DS5% and SL5%) ( $w/v$ ) of each crude extract. All of the coated panels were firmly tied-up on the stainless-steel frame using iron wire and were immersed in the seawater, about 2 m from the bottom of the ocean for both immersion sites, which were Kemaman and Pulau Redang. Figure 11 shows that the tested panels for Kemaman (Figure 11A) and Pulau Redang (Figure 11B) were retrieved and photographed at different time intervals, respectively. A comparison of the blank panel and antifouling paint panels in the seawater at Kemaman and Pulau Redang on week five are shown in Figure 12. It was observed that macroalgae grew heavily on the blank panels. However, significantly less macroalgae were found growing on the antifouling paint coated with the SL5%, DS5%, and DS10% panels. The antimacrofouling of the lower concentrations showed greater antifouling activity compared to the higher concentrations. This could be correlated with the crystal violet assay and antibiofilm data in aquarium testing in the current study as the biofilm inhibition showed higher activity when lower concentrations were used. No attachment of barnacles was found on the antifouling paints incorporated with the crude extracts. The panels coated with the formulated antifouling paint are comparable to the standard commercially available paints, which were used as a positive control, as both antifouling paints and commercial antifouling paint can reduce the attachment of macrofoulers on the tested panels. Previously, Soliman et al. [11] developed natural antifouling paint by incorporating crude extracts of soft corals into the base paint for controlling the growth of biofoulers. Hamdona et al. [55] reported that the crude extracts of marine algae showed the best antifouling activity against micro- and macro-fouling when submerged in seawater over 140 days. These results suggest that the panels coated with antifouling paint incorporated with *D. setosum* and *S. lanceolata* crude extracts were effective in controlling biofouling formation over a short period in the marine environment.



(A)



(B)

**Figure 11.** Underwater images of different coated panels in the seawater at Kemaman (A) and Pulau Redang (B). Panel coated with blank paint (BL); Panel coated with commercial antifouling paint (RF1 and RF2); DS5% and DS10% (*w/v*): Paint with *D. setosum* crude extract; SL5% and SL10% (*w/v*): Paint with *S. lanceolata* crude extract.



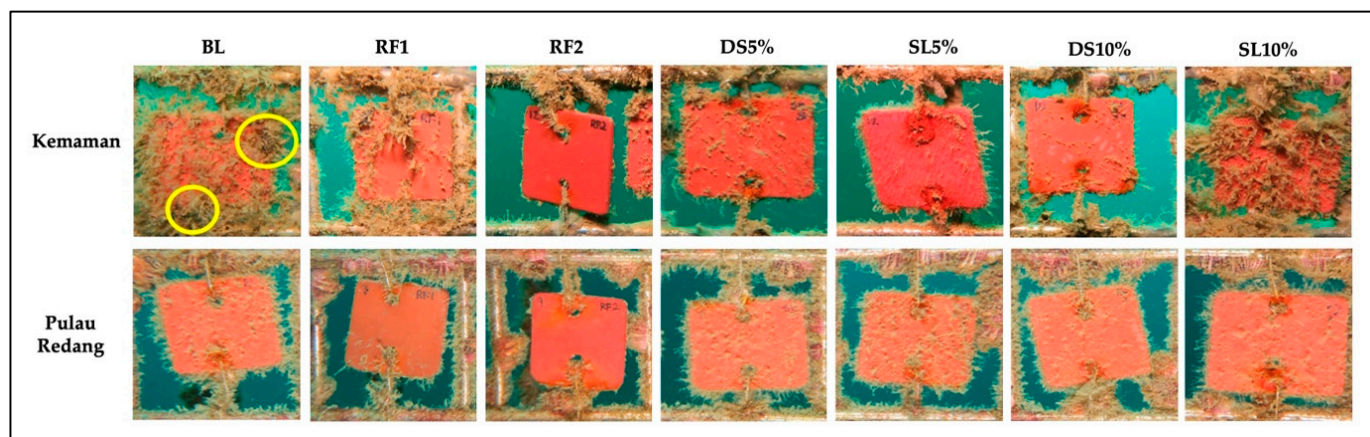


**Figure 12.** Underwater images of different coated panels in the seawater for five weeks at Kemaman and Pulau Redang. BL: Panel coated with blank paint (control); Panel coated with commercial antifouling paint (RF1 and RF2); DS5% and DS10% (*w/v*): Paint with *D. setosum* crude extract; SL5% and SL10% (*w/v*): Paint with *S. lanceolata* crude extract. Yellow circles indicate the attachment of barnacles on the surface of the blank paint panel.

#### 4. Conclusions

*S. lanceolata* and *D. setosum* paint extracts were found to have antifouling properties against *P. aeruginosa*. Metabolite profiling from both of these crude extracts was achieved through a metabolomic technique using a different type of software. The findings from the current study indicate that bioactive compounds isolated using HRESI-LCMS with the known compounds of more than 20 compounds from the samples of both *D. setosum* and *S. lanceolata* might have the potential to be developed as an antifouling agent. The incorporation of these crude extracts into the paint revealed the antifouling activities of the paints in the laboratory and field testing.

**Supplementary Materials:** The following supporting information can be downloaded at: <https://www.mdpi.com/article/10.3390/jmse11030602/s1>, Supplementary Tables S1 and S2 related to the spectra of the compounds presented in *D. setosum* and *S. lanceolata* (HRESI-LCMS).

**Author Contributions:** Conceptualization, N.I., K.B. (Kesavan Bhubalan), N.W.M. and F.A.; investigation, M.M.R., N.I.A.R., N.N.R., J.Y.F.S., K.B. (Kamariah Bakar), N.A.M.Z., A.K.A. and N.I.; resources, N.I., K.B. (Kesavan Bhubalan), N.W.M. and F.A.; validation, N.I. and A.K.A.; formal analysis, M.M.R., N.I.A.R., N.N.R. and A.K.A.; writing—original draft preparation, M.M.R., N.I.A.R., N.N.R., J.S., M.D.-D., A.K.A. and N.I.; writing—review and editing, M.M.R., N.I.A.R., N.N.R., J.S., M.D.-D., A.K.A. and N.I.; supervision, N.I.; project administration, N.I.; funding acquisition, N.I. All authors have read and agreed to the published version of the manuscript.

**Funding:** This research was financially supported local Oil and Gas Company (Bandar Baru Bangi, Selangor, Malaysia), grant number 63931.

**Institutional Review Board Statement:** Not applicable.

**Informed Consent Statement:** Not applicable.

**Data Availability Statement:** The data are available upon request.

**Conflicts of Interest:** The authors declare no conflict of interest.

#### References

1. Dahms, H.U.; Dobretsov, S. Antifouling Compounds from Marine Macroalgae. *Mar. Drugs* **2017**, *15*, 265. [[CrossRef](#)] [[PubMed](#)]
2. Ciriminna, R.; Bright, F.V.; Pagliaro, M. Ecofriendly Antifouling Marine Coatings. *ACS Sustain. Chem. Eng.* **2015**, *3*, 559–565. [[CrossRef](#)]
3. Kyei, S.K.; Darko, G.; Akaranta, O. Chemistry and Application of Emerging Ecofriendly Antifouling Paints: A Review. *J. Coat. Technol. Res.* **2020**, *17*, 315–332. [[CrossRef](#)]

4. Palanichamy, S.; Subramanian, G. Antifouling Properties of Marine Bacteriocin Incorporated Epoxy Based Paint. *Prog. Org. Coat.* **2017**, *103*, 33–39. [[CrossRef](#)]
5. Viju, N.; Punitha, S.M.J.; Satheesh, S. Antifouling Properties of Bacteria Associated with Marine *Oyster crassostrea* sp. *Thalassas* **2018**, *34*, 471–482. [[CrossRef](#)]
6. Satheesh, S.; Ba-Akdah, M.A.; Al-Sofyani, A.A. Natural Antifouling Compound Production by Microbes Associated with Marine Macroorganisms—A Review. *Electron. J. Biotechnol.* **2016**, *21*, 26–35. [[CrossRef](#)]
7. Tian, L.; Yin, Y.; Jin, H.; Bing, W.; Jin, E.; Zhao, J.; Ren, L. Novel Marine Antifouling Coatings Inspired by Corals. *Mater. Today Chem.* **2020**, *17*, 100924. [[CrossRef](#)]
8. Rattaya, S.; Benjakul, S.; Prodpran, T. Extraction, Antioxidative, and Antimicrobial Activities of Brown Seaweed Extracts, *Turbinaria Ornata* and *Sargassum Polycystum*, Grown in Thailand. *Int. Aquat. Res.* **2015**, *7*, 1–16. [[CrossRef](#)]
9. Rima, M.; Trognon, J.; Latapie, L.; Chbani, A.; Roques, C.; Garah, F. el Seaweed Extracts: A Promising Source of Antibiofilm Agents with Distinct Mechanisms of Action against *Pseudomonas Aeruginosa*. *Mar. Drugs* **2022**, *20*, 92. [[CrossRef](#)]
10. Lhullier, C.; Moritz, M.I.G.; Tabalipa, E.O.; Sardá, F.N.; Schneider, N.F.Z.; Moraes, M.H.; Constantino, L.; Reginatto, F.H.; Steindel, M.; Pinheiro, U.S.; et al. Biological Activities of Marine Invertebrates Extracts from the Northeast Brazilian Coast. *Braz. J. Biol.* **2020**, *80*, 393–404. [[CrossRef](#)]
11. Soliman, Y.A.A.; Brahim, A.M.; Moustafa, A.H.; Hamed, M.A.F. Antifouling Evaluation of Extracts from Red Sea Soft Corals against Primary Biofilm and Biofouling. *Asian Pac. J. Trop. Biomed.* **2017**, *7*, 991–997. [[CrossRef](#)]
12. Patro, S.; Adhavan, D.; Jha, S. Fouling Diatoms of Andaman Waters and Their Inhibition by Spinal Extracts of the Sea Urchin *Diadema Setosum* (Leske, 1778). *Int. Biodeterior. Biodegrad.* **2012**, *75*, 23–27. [[CrossRef](#)]
13. Nandhini, S.; Revathi, K. Antifouling Activity of Extracts from Mangroves against Biofouling Bacteria Isolated from Boats in Royapuram, Chennai, India. *Int. J. Curr. Microbiol. Appl. Sci.* **2016**, *5*, 324–335. [[CrossRef](#)]
14. Murzina, S.A.; Dgebuadze, P.Y.; Pekkoeva, S.N.; Voronin, V.P.; Mekhova, E.S.; Thanh, N.T.H. Lipids and Fatty Acids of the Gonads of Sea Urchin *Diadema Setosum* (Echinodermata) From the Coastal Area of the Nha Trang Bay, Central Vietnam. *Eur. J. Lipid Sci. Technol.* **2021**, *123*, 2000321. [[CrossRef](#)]
15. Yusuf, M.; Fitriani Nur, U.A.; Rifai, A. In Vitro Antibacterial Activity and Potential Applications in Food of Sea Urchin (*Diadema Setosum*) from Cape of Palette, South Sulawesi. *Food Res* **2020**, *4*, 2139–2146. [[CrossRef](#)]
16. Marimuthu, K.; Gunaselvam, P.; Rahman, M.A.; Xavier, R.; Arockiaraj, J.; Subramanian, S.; Yusoff, F.M.; Arshad, A. Antibacterial Activity of Ovary Extract from Sea Urchin *Diadema Setosum*. *Eur. Rev. Med. Pharmacol. Sci.* **2015**, *19*, 1895–1899.
17. Sabilu, Y.; Jafriati, M.R. Test of Bioactivity and Antioxidant Activity of Sea Urchin (*Diadema setosum*) Gonads As Medicinal Ingredients Based on Marine Biodiversity. *J. Southwest Jiaotong Univ.* **2022**, *57*, 147–153. [[CrossRef](#)]
18. Sachithanandam, V.; Lalitha, P.; Parthiban, A.; Mageswaran, T.; Manmadhan, K.; Sridhar, R. A Review on Antidiabetic Properties of Indian Mangrove Plants with Reference to Island Ecosystem. *Evid. Based Complement. Altern. Med.* **2019**, *2019*, 4305148. [[CrossRef](#)]
19. Eswaraiyah, G.; Peele, K.A.; Krupanidhi, S.; Kumar, R.B.; Venkateswarulu, T.C. Studies on Phytochemical, Antioxidant, Antimicrobial Analysis and Separation of Bioactive Leads of Leaf Extract from the Selected Mangroves. *J. King Saud Univ. Sci.* **2020**, *32*, 842–847. [[CrossRef](#)]
20. Abeysinghe, P.D. Antibacterial Activity of Some Medicinal Mangroves against Antibiotic Resistant Pathogenic Bacteria. *Indian J. Pharm. Sci.* **2010**, *72*, 167–172. [[CrossRef](#)]
21. Kokpol, U.; Chittawong, V.; Miles, D.H. Chemical Constituents of the Roots of *Acanthus Illicifolius*. *J. Nat. Prod.* **1986**, *49*, 355–356. [[CrossRef](#)]
22. Chandrasekaran, M.; Kannathan, K.; Venkatesalu, V.; Prabhakar, K. Antibacterial Activity of Some Salt Marsh Halophytes and Mangrove Plants against Methicillin Resistant *Staphylococcus Aureus*. *World. J. Microbiol. Biotechnol.* **2009**, *25*, 155–160. [[CrossRef](#)]
23. Bandaranayake, W.M. Traditional and Medicinal Uses of Mangroves. *Mangroves Salt Marshes* **1998**, *2*, 133–148. [[CrossRef](#)]
24. Agoramoorthy, G.; Chandrasekaran, M.; Venkatesalu, V.; Hsu, M.J. Antibacterial and Antifungal Activities of Fatty Acid Methyl Esters of the Blind-Your-Eye Mangrove from India. *Braz. J. Microbiol.* **2007**, *38*, 739–742. [[CrossRef](#)]
25. Bandaranayake, W.M. Bioactivities, Bioactive Compounds and Chemical Constituents of Mangrove Plants. *Wetl. Ecol. Manag.* **2002**, *10*, 421–452. [[CrossRef](#)]
26. Ragavan, P.; Ravichandran, K.; Mohan, P.M.; Sxaena, A.; Prasanth, R.S.; Jayaraj, R.S.C.; Saravanan, S. Short Communication: New Distributional Records of *Sonneratia* Spp. from Andaman and Nicobar Islands, India. *Biodiversitas* **2014**, *15*, 251–260. [[CrossRef](#)]
27. Qiu, S.; Zhou, R.C.; Li, Y.Q.; Havanond, S.; Jaengjai, C.; Shi, S.H. Molecular Evidence for Natural Hybridization between *Sonneratia Alba* and *S. Griffithii*. *J. Syst. Evol.* **2008**, *46*, 391–395. [[CrossRef](#)]
28. El-Sayed, W.M.M.; Elshaer, M.M.; Ibrahim, H.A.H.; El-Metwaly, M.E.A. Antimicrobial Agents from Sea Urchin (*Diadema Setosum*) Collected from the Red Sea, Egypt. *Egypt J. Aquat. Biol. Fish.* **2020**, *24*, 33–51. [[CrossRef](#)]
29. Andriani, Y.; Tengku-Muhammad, T.S.; Mohamad, H.; Saidin, J.; Syamsudin, D.F.; Chew, G.S.; Wahid, M.E.A. *Phaleria Macrocarpa* Boerl. (Thymelaeaceae) Leaves Increase SR-BI Expression and Reduce Cholesterol Levels in Rats Fed a High Cholesterol Diet. *Molecules* **2015**, *20*, 4410–4429. [[CrossRef](#)]
30. Azemi, A.K.; Mokhtar, S.S.; Sharif, S.E.T.; Rasool, A.H.G. *Clinacanthus Nutans* Attenuates Atherosclerosis Progression in Rats with Type 2 Diabetes by Reducing Vascular Oxidative Stress and Inflammation. *Pharm. Biol.* **2021**, *59*, 1432–1440. [[CrossRef](#)]

31. Mazlan, N.W.; Tate, R.; Yusoff, Y.M.; Clements, C.; Edrada-Ebel, R. Metabolomics-Guided Isolation of Anti-Trypanosomal Compounds from Endophytic Fungi of the Mangrove Plant *Avicennia Lanata*. *Curr. Med. Chem.* **2019**, *27*, 1815–1835. [[CrossRef](#)] [[PubMed](#)]
32. Macintyre, L.; Zhang, T.; Viegelmann, C.; Martinez, I.J.; Cheng, C.; Dowdells, C.; Abdelmohsen, U.R.; Gernert, C.; Hentschel, U.; Edrada-Ebel, R.A. Metabolomic Tools for Secondary Metabolite Discovery from Marine Microbial Symbionts. *Mar. Drugs* **2014**, *12*, 3416–3448. [[CrossRef](#)] [[PubMed](#)]
33. Abdelmohsen, U.R.; Cheng, C.; Viegelmann, C.; Zhang, T.; Grkovic, T.; Ahmed, S.; Quinn, R.J.; Hentschel, U.; Edrada-Ebel, R.A. Dereplication Strategies for Targeted Isolation of New Antitrypanosomal Actinosporins a and B from a Marine Sponge Associated-Actinokineospora Sp. EG49. *Mar. Drugs* **2014**, *12*, 1220–1244. [[CrossRef](#)] [[PubMed](#)]
34. Noor Idora, M.S.; Ferry, M.; Wan Nik, W.B.; Jasnizat, S. Evaluation of Tannin from *Rhizophora Apiculata* as Natural Antifouling Agents in Epoxy Paint for Marine Application. *Prog. Org. Coat.* **2015**, *81*, 125–131. [[CrossRef](#)]
35. Salama, A.J.; Satheesh, S.; Balqadi, A.A. Antifouling Activities of Methanolic Extracts of Three Macroalgal Species from the Red Sea. *J. Appl. Phycol.* **2018**, *30*, 1943–1953. [[CrossRef](#)]
36. Leroy, C.; Delbarre, C.; Ghillebaert, F.; Compere, C.; Combes, D. Effects of Commercial Enzymes on the Adhesion of a Marine Biofilm-Forming Bacterium. *Biofouling* **2008**, *24*, 11–22. [[CrossRef](#)]
37. Chen, L.; Xia, C.; Qian, P.Y. Optimization of Antifouling Coatings Incorporating Butenolide, a Potent Antifouling Agent via Field and Laboratory Tests. *Prog. Org. Coat.* **2017**, *109*, 22–29. [[CrossRef](#)]
38. Viju, N.; Satheesh, S.; Punitha, S.M.J. Antifouling Activities of Antagonistic Marine Bacterium *Pseudomonas Putida* Associated with an Octopus. *Proc. Natl. Acad. Sci. India Sect. B Biol. Sci.* **2017**, *87*, 1113–1124. [[CrossRef](#)]
39. Kitagawa, I.; Hamamoto, Y.; Kobayashi, M. Sulfonoglycolipid from the Sea Urchin *Anthocidaris Crassispina* a. Agassiz. *Chem Pharm Bull.* **1979**, *27*, 1394–1397. [[CrossRef](#)]
40. Yende, S.; Harle, U.; Chaugule, B. Therapeutic Potential and Health Benefits of *Sargassum* species. *Pharmacogn. Rev.* **2014**, *8*, 1–7. [[CrossRef](#)]
41. Plouguerné, E.; da Gama, B.A.P.; Pereira, R.C.; Barreto-Bergter, E. Glycolipids from Seaweeds and Their Potential Biotechnological Applications. *Front. Cell. Infect. Microbiol.* **2014**, *4*, 174. [[CrossRef](#)]
42. Arunkumar, K.; Selvapalam, N.; Rengasamy, R. The Antibacterial Compound Sulphoglycerolipid 1-0 Palmitoyl-3-0(6-Sulpho- $\alpha$ -Quinovopyranosyl)-Glycerol from *Sargassum Wightii* Greville (Phaeophyceae). *Bot. Mar.* **2005**, *48*, 441–445. [[CrossRef](#)]
43. Bakar, K.; Mohamad, H.; Latip, J.; Seng Tan, H.; Gan, A.; Heng, M. Fatty Acids Compositions of *Sargassum granuliferum* and *Dictyota dichotoma* and Their Anti-Fouling Activities. *J. Sustain. Sci. Manag.* **2017**, *12*, 8–16.
44. Bhattarai, H.D.; Yoo, K.L.; Kyeung, H.C.; Hong, K.L.; Hyun, W.S. The Study of Antagonistic Interactions among Pelagic Bacteria: A Promising Way to Coin Environmental Friendly Antifouling Compounds. *Hydrobiologia* **2006**, *568*, 417–423. [[CrossRef](#)]
45. Fusetani, N. Biofouling and Antifouling. *Nat. Prod. Rep.* **2004**, *21*, 94–104. [[CrossRef](#)] [[PubMed](#)]
46. Almeida, J.R.; Correia-Da-Silva, M.; Sousa, E.; Antunes, J.; Pinto, M.; Vasconcelos, V.; Cunha, I. Antifouling Potential of Nature-Inspired Sulfated Compounds. *Sci. Rep.* **2017**, *7*, 42424. [[CrossRef](#)]
47. Petitbois, J.G. Antifouling Compounds from Two Red Sea Organisms: A *Hyrtios* Sp. Sponge and an *Okeania* Sp. Cyanobacterium. Ph.D. Thesis, Hokaido University, Sapporo, Japan, 2018.
48. Han, S.; Hanh Nguyen, T.T.; Hur, J.; Kim, N.M.; Kim, S.B.; Hwang, K.H.; Moon, Y.H.; Kang, C.; Chung, B.; Kim, Y.M.; et al. Synthesis and Characterization of Novel Astragalin Galactosides Using  $\beta$ -Galactosidase from *Bacillus Circulans*. *Enzym. Microb. Technol.* **2017**, *103*, 59–67. [[CrossRef](#)]
49. González, A.G.; Alvarenga, N.L.; Ravelo, A.G.; Bazzocchi, I.L.; Ferro, E.A.; Navarro, A.G.; Moujir, L.M. Scutione, a New Bioactive Norquinonemethide Triterpene from *Maytenus Scutioides* (Celastraceae). *Bioorg. Med. Chem.* **1996**, *4*, 815–820. [[CrossRef](#)]
50. Cheriet, T.; Mancini, I.; Seghiri, R.; Benayache, F.; Benayache, S. Chemical Constituents and Biological Activities of the Genus *Linaria* (Scrophulariaceae). *Nat. Prod. Res.* **2015**, *29*, 1589–1613. [[CrossRef](#)]
51. Rogers, T.O.; Birnbaum, J. Biosynthesis of Fosfomycin by *Streptomyces Fradiae*. *Antimicrob. Agents Chemother.* **1974**, *5*, 121–132. [[CrossRef](#)]
52. Hendlin, D.; Stapley, E.O.; Jackson, M.; Wallick, H.; Miller, A.K.; Wolf, F.J.; Miller, T.W.; Chaiet, L.; Kahan, F.M.; Foltz, E.L.; et al. Phosphonomycin, a New Antibiotic Produced by Strains of *Streptomyces*. *Science (1979)* **1969**, *166*, 122–123. [[CrossRef](#)] [[PubMed](#)]
53. de Simeis, D.; Serra, S. Actinomycetes: A Never-Ending Source of Bioactive Compounds—An Overview on Antibiotics Production. *Antibiotics* **2021**, *10*, 483. [[CrossRef](#)]
54. Viju, N.; Punitha, S.M.J.; Satheesh, S. Antifouling Potential of Palmyra Palm (*Borassus Flabellifer*) Fruit Husk Extract. *Proc. Natl. Acad. Sci. India Sect. B Biol. Sci.* **2020**, *90*, 1005–1015. [[CrossRef](#)]
55. Samia, K. Hamdona, S.; Abo Taleb, A.; Salem, D.; Tadros, H. Fouling Control by New Egyptian Natural Sources in Marine Aquaculture. *J. Chem. Biol. Phys. Sci.* **2019**, *9*, 92–105. [[CrossRef](#)]

**Disclaimer/Publisher’s Note:** The statements, opinions and data contained in all publications are solely those of the individual author(s) and contributor(s) and not of MDPI and/or the editor(s). MDPI and/or the editor(s) disclaim responsibility for any injury to people or property resulting from any ideas, methods, instructions or products referred to in the content.